The *Helicobacter pylori* biofilm involves a multi-gene stress-biased response including a structural role for flagella

Skander Hathroubi[#], Julia Zerebinski and Karen M. Ottemann

Department of Microbiology and Environmental Toxicology, University of California, Santa Cruz, California, 95060 USA

Running title: Structural role of flagella in *H. pylori biofilm*

#Corresponding Author:

[#]Address correspondence to Skander Hathroubi, shathrou@ucsc.edu. 1156 High Street, METX. Santa Cruz, CA 95064

ABSTRACT

Helicobacter pylori has an impressive ability to persist chronically in the human stomach. Similar characteristics are associated with biofilm formation in other bacteria. The *H. pylori* biofilm process, however, is poorly understood. To gain insight into this mode of growth, we carried out comparative transcriptomic analysis between *H. pylori* biofilm and planktonic cells, using the mouse colonizing strain SS1. Optimal biofilm formation was obtained with low serum and three-day growth, conditions which caused both biofilm and planktonic cells to be ~80% coccoid. RNA-seq analysis found that 8.18% of genes were differentially expressed between biofilm and planktonic cell transcriptomes. Biofilm-downregulated genes included those involved in metabolism and translation, suggesting these cells have low metabolic activity. Biofilm-upregulated genes included those whose products were predicted to be at the cell envelope, involved in regulating a stress response, and surprisingly, genes related to formation of the flagellar apparatus. Scanning electron microscopy visualized flagella that appeared to be a component of the biofilm matrix, supported by the observation that an aflagellated mutant displayed a less robust biofilm with no apparent filaments. We observed flagella in the biofilm matrix of additional *H. pylori* strains, supporting that flagellar use is widespread. Our data thus supports a model in which *H. pylori* biofilm involves a multi-gene stress-biased response, and that flagella play an important role in *H. pylori* biofilm formation.

IMPORTANCE

Biofilms, communities of bacteria that are embedded in a hydrated matrix of extracellular polymeric substances, pose a substantial health risk and are key contributors to many chronic and recurrent infections. Chronicity and recalcitrant infections are also common features associated with the ulcer-causing human pathogen *H. pylori.* However, relatively little is known about the role of biofilms in *H. pylori* pathogenesis as well as the biofilm structure itself and the genes associated with this mode of growth. In the present study, we found that *H. pylori* biofilm cells highly expressed genes related to cell envelope, stress response and those encoding the flagellar apparatus. Flagellar filaments were seen in high abundance in the biofilm. Flagella are known to play a role in initial biofilm formation, but typically are downregulated after that state. *H. pylori* instead appears to have co-opted these structures for non-motility roles, including a role building a robust biofilm.

KEYWORDS

Helicobacter pylori, biofilm, flagella, stress, metabolism, RNA-seq, transcriptome

INTRODUCTION

H. pylori has been co-evolving with humans for tens of thousands of years (1). During this time, it has adapted to survive the hostile environment of the stomach and evade the immune system, allowing it to persist for the life of the host (2). *H. pylori* colonizes gastric epithelial surfaces and within the thin layer of mucus near the cells (3). More recently, *H. pylori* was found to colonize within gastric glands, repeated invaginations of the gastrointestinal tract, which may provide the bacteria a favorable niche (4, 5). Even though most infections are asymptomatic, *H. pylori* persistence is considered a major risk factor for gastric and duodenal ulcers, gastric Mucosa-Associated Lymphoid Tissue (MALT) lymphoma, and gastric adenocarcinoma (6). *H. pylori* infections remain difficult to treat, and when left untreated (7), 1-2% progress to gastric cancer (8, 9).

H. pylori possesses several mechanisms to escape the challenging environment of the stomach where the pH is around 2. These include urease production, flagellar motility, and chemotaxis, which are all required for the initial and sustained colonization of the gastric epithelial surface (10). Urease catalyzes the hydrolysis of urea, which is abundant in stomach, into bicarbonate and ammonia and thus raises the pH to near neutral (10). pH elevation decreases the viscoelastic properties of mucus gel and improves the motility of *H. pylori*, which can then swim away from the lumen to reach safer niches including those close to the gastric epithelial surface (11). *H. pylori* forms microcolonies at the cell surface *in vitro* (12, 13) as well as within gastric glands (5). This microcolony mode of growth may be consistent with the bacteria being in a biofilm-growth mode.

Biofilms are dense aggregates of microorganisms attached to a surface and embedded in an extracellular polymeric matrix (14). In contrast with the other mode of bacterial growth, free-

floating or planktonic, biofilm cells tend to be more tolerant towards antimicrobials and host immune responses (14, 15). Biofilms are also frequently associated with chronic disease including pneumonia in cystic fibrosis patients, Lyme disease, and chronic otitis media (16-18). In those chronic diseases, biofilm growth is considered to be a survival strategy used by pathogens to escape antimicrobial therapies, avoid clearance by the immune system, and to persist for the lifetime of the host.

Chronicity and recalcitrant infections are also common features associated with *H. pylori* (19). Yet, the role of biofilm growth in promoting *H. pylori* persistence is still not clear (20). The first suggestion of biofilm formation by *H. pylori* during colonization of the human gastric mucosa was found using biopsies and scanning electron microscopy (SEM) analysis (20-22). These studies demonstrated that gastric biopsy samples from *H. pylori*-positive patients showed dense layers of bacteria aggregated and attached to the mucosal surface. The bacteria were consistent in appearance to *H. pylori* with cells in both the spiral and coccoid morphologies. The same bacterial-appearing structures were absent in *H. pylori*-negative patients, however there has not yet been conclusive evidence showing that *H. pylori* forms a biofilm *in vivo*.

H. pylori has been well documented to form a biofilm *in vitro*. The first report of *in vitro* biofilm formation by *H. pylori* was described to occur in clinical, laboratory, and mouse-adapted strains, and was observed at the air-liquid interface on glass coverslips when the bacteria were grown in Brucella broth (BB) supplemented with slightly lower than normal fetal bovine serum (FBS) (23). The biofilms were mainly composed of coccoid bacteria, with a minority of spiral and rod shaped ones (23). In subsequent reports, scientists analyzed the extracellular polymeric substance (EPS) of *H. pylori* biofilms and found proteomannans, LPS-related structures, extracellular DNA, proteins, and outer membrane vesicles (24, 25).

106 Additionally, biofilm cells have been shown to exhibit high resistance *in vitro* to
107 clarithromycin, which is one of the common antibiotics used to treat *H. pylori* infection (26). The
108 minimum inhibitory concentration (MIC) and the minimum bactericidal concentration (MBC)
109 were increased by 16-and 4-fold, respectively, in the biofilm cells as compared to planktonic
110 ones (26). However, despite the growing evidences of *H. pylori* biofilm formation both *in vitro*
111 and *in vivo* (20-22, 24), little is known about the genes involved in biofilm formation. We thus
112 sought to characterize *H. pylori* biofilm and investigate global transcriptional changes during
113 biofilm formation, with a particular focus on *H. pylori* strain SS1 because it is able to colonize
114 mice and thus will be able to serve as a model for biofilm formation *in vivo*.

RESULTS

Biofilm formation and growth condition. *H. pylori* strain SS1 has been extensively used as a murine model of *H. pylori* infection. *H. pylori* SS1 biofilms, however, are difficult to detect when the bacteria are grown in standard nutrient-rich media routinely used for *H. pylori* culture. A previous study reported that *H. pylori* biofilm formation was significantly dependent on the growth media used (27). We thus evaluated the ability of the *H. pylori* SS1 strain to form a biofilm using the crystal violet biofilm assay, and bacteria grown under varying growth conditions that included different growth media, incubation times, and concentrations of serum.

Using Brucella Broth (BB) media supplemented with 10% FBS (BB10), the condition usually used for *H. pylori* liquid growth, no biofilm was detected. We therefore explored lower amounts of serum, as these have been reported elsewhere to promote adhesion of *H. pylori* strain 26695 (28) and biofilm formation of reference *H. pylori* strain ATCC 43629 and clinical strains *H. pylori* 9/10 (27). While only a slight biofilm was observed when *H. pylori* SS1 strain was grown with BB supplemented with 6% FBS, a pronounced biofilm ($p< 0.01$) was detected in BB supplemented with 2% FBS (BB2) (Fig. 1A). The *H. pylori* growth rate was slightly reduced in BB2 compared with BB10, which suggests that the increase of biofilm formation was not due to increased growth (data not shown). HAMs F12 similarly only supported biofilm formation with low FBS percentages (Fig. 1B). Further experiments identified that three days of growth in BB2 led to the greatest amount of biofilm (Fig. 1C). These results thus suggest that BB media supplemented with 2% serum and growth for three days is an optimal condition for studying *H. pylori* SS1 biofilm formation.

Biofilm characterization. To confirm and extend the results obtained with the crystal violet biofilm assay, biofilms of *H. pylori* SS1 were visualized by confocal laser scanning microscopy (CLSM) and staining with FilmTracer™ FM®1–43, a dye that fluoresces once inserted into the cell membrane. After three days of growth in BB2, we observed a thick bacterial biomass that non-homogeneously covered the surface, consistent with a well-developed biofilm (Fig. 2). Using z-stack images, the thickness of the *H. pylori* SS1 biofilm was determined to be 11.64 ± 2.63 $\mu m^3/\mu m$ (Supplementary Movie 1). As expected, *H. pylori* SS1 grown in BB10 did not form a biofilm that could be visualized with CLSM (data not shown).

To further characterize the EPS that composed the SS1 biofilm matrix, BOBO-3 and FilmTracer SYPRO Ruby biofilm matrix stains were used to stain extracellular DNA (eDNA) and extracellular proteins, respectively as described previously (29, 30). Both of these molecules extensively stained the biofilm EPS, consistent with the idea that the *H. pylori* SS1 biofilm matrix contains significant amount of eDNA and extracellular proteins (Fig. 2B and C). Because these same molecules have been detected in other *H. pylori* strains, these results suggest that the *H. pylori* EPS is typically composed of eDNA and proteins (24, 31).

We also performed live-dead staining with the FilmTracer LIVE/DEAD biofilm viability kit, to define whether the biofilm cells were alive or dead. This approach revealed a subpopulation of dead or damaged cells, stained red, that appear to be homogeneously distributed within the live biofilm cells, which stained green (Fig. 2D-F). This result suggests that the *H. pylori* biofilm contains both live and dead cells.

To determine the importance of extracellular proteins and eDNA in the biofilm matrix of *H. pylori* SS1, we employed enzymatic treatment using DNAse I and proteinase K. Proteinase K treatment significantly dispersed pre-formed biofilms ($P < 0.01$) (Fig. 3). *H. pylori* pre-formed

biofilms were, however, resistant to DNase treatments. These data suggest that DNA may play only a minor role in the biofilm matrix, however, extracellular proteins likely play an important role in the biofilm architecture of *H. pylori*, as has been reported in other *H. pylori* strains (24, 31). These results suggest that many *H. pylori* strains, including SS1, use a protein-based biofilm matrix.

Transcriptomic profiling of biofilm versus planktonic cells. To gain insight into the genes involved in *H. pylori* biofilm growth, we performed a transcript profiling experiment using RNA-seq. For this experiment, we grew *H. pylori* SS1 in BB2 in six well plates for three-days, and collected the free-floating planktonic cells and the bottom-attached biofilm ones from the same wells. We collected RNA from three biological replicates grown on two separate days. A total of 10-20 million reads per sample was generated by RNA-seq. These reads were then mapped to *H. pylori* SS1 complete reference genome (32), and revealed a clear clustering of the biofilm-grown cells in a distinct population compared to the planktonic ones (Fig. 4A). This transcriptomic analysis showed that 122 of 1491 genes (8.18%) were significantly differentially expressed ($p< 0.01$ and $\log_2$-fold change >1 or <-1) between *H. pylori* biofilm and planktonic populations (Fig. 4B and Fig. 5). 61 genes were significantly upregulated in biofilm cells compared to their planktonic counterparts, while another 61 were significantly upregulated in planktonic cells (Table 2 and 3). To validate the results obtained by this RNA-seq, the relative abundance of selected RNA transcripts was quantified by quantitative RT-PCR (qRT-PCR). Using this approach, we detected the same gene expression trend between qRT-PCR and RNA-seq, thus validating our results (Fig. 6). Below we discuss the most prominent of these genes, and what they suggest about the *H. pylori* biofilm growth state.

Our data suggest that biofilm cells may be less metabolically active than planktonic cells, based on the decreased expression of several genes involved in translation and ribosomal structure (Fig. 5, Table 3). Similarly, genes involved in metabolism, biosynthesis of cofactors, and urease were also down-regulated (Fig. 5, Table 3).

We found evidence that biofilms cells experience a stressful environment. Indeed, genes coding for several stress response-related genes such as *hrcA*, *hspR*, *crdR*, *recR* and *pgdA* were up-regulated in biofilm cells (Table 2). The *hspR* and *hrcA* genes code for transcriptional repressor proteins belonging to the heat shock protein family, and were both up-regulated in biofilm cells. The *crdR* gene, which encodes a copper-related transcriptional response regulator was also up-regulated in *H. pylori* biofilm cells. Several transcripts encoding for oxidative stress resistance were similarly up-regulated in biofilm cells. These included *recR*, a gene encoding for a DNA recombination protein, as well as *pgdA* which encodes for a peptidoglycan deacetylase. These have both been previously associated with oxidative stress in *H. pylori* (33).

We found that the ATP-dependent protease HslV gene was among the most down-regulated genes in *H. pylori* biofilm (Table 3). Although this protein has not yet been studied in the context of *H. pylori* biofilms, the orthologous *E. coli* HslV protease has been previously associated with biofilm dispersal (34).

Our data suggest that biofilm cells may be less virulent in some ways, but more in others. Transcripts coding for some *H. pylori* virulence, colonization or immunogenic factors were low in biofilm cells, including the UreA subunit of urease, the GroEL chaperone, and the HcpC cysteine rich protein. These have each been shown to play roles in colonization or promoting inflammatory gene expression (35-37). On the other hand, only three genes encoded within the cytotoxin-associated gene pathogenicity island (*cag*PAI) (38, 39) *cagL*, *cagW* and *cagE* were

207 significantly highly expressed in biofilm cells of *H. pylori*. These genes are in separate operons
208 (38), and encode for cag pathogenicity island protein CagL/Cag18, an integrin binding protein at
209 the cag pilus tip, cag pathogenicity island protein CagW/Cag10 and type IV secretion system
210 protein CagE/virB4, both part of the inner membrane protein transfer complex (39).

211 Many genes related to the cell envelope were up-regulated in biofilm cells (Fig. 5).
212 Indeed, genes coding for proteins involved in lipopolysaccharide synthesis such as *lpxB*, which
213 encodes a lipid-A disaccharide synthase, and *lptB*, which encodes a lipopolysaccharide export
214 system ATPase, were up-regulated in biofilm cells (Table 2). Numerous transcripts encoding
215 cytoplasmic and outer membrane proteins were also elevated in biofilm cells (i.e. *homC*, *homD*
216 and HPYLSS1_00450) (Table 2).

217 Interestingly, the majority of the upregulated cell envelope genes in biofilm cells encoded
218 for flagellar structure and biosynthesis proteins such as *flgL*, *flgK*, *fliD* and *flgE*, which encode
219 for flagellar hook-associated proteins (Table 2). Two known or putative flagellin genes, *flaB* and
220 *flaG* were also upregulated in the biofilms (Table 2). These data suggested the intriguing idea
221 that flagella might play a role in the *H. pylori* biofilm.

222

223 ***Flagella are present and play a structural role in H. pylori biofilms.*** The transcriptomic data
224 above suggested that flagellar components are upregulated in the biofilm cells, so we used SEM
225 to gain insights into the biofilm architecture of *H. pylori*. This analysis demonstrated three-
226 dimensional structures composed of bacterial cells adherent to one another and to the surface
227 (Fig. 7A). Biofilms contained mainly coccoid cells along with some rod-shaped cells (Fig. 7A),
228 as described previously for *H. pylori* biofilms (20-23). When compared to planktonic

229 populations, the proportion of both morphologies were similar at ~ 80% coccoid cells (data not
230 shown).

231 Interestingly, extensive networks of bundles of filaments were visible in the biofilms.
232 In some cases, these appeared to be connected to the bacterial pole, as would be expected for
233 flagella (Fig. 7A, arrowheads). We measured the dimensions of the filaments to see if they were
234 consistent in size with flagella. The width and the length measured at 20 to 30nm and 3 to 4μm,
235 respectively, and were in agreement with those reported previously for *H. pylori* flagella (40).
236 This data, especially when combined with transcriptomics, suggested these structures could be
237 flagella. We therefore analyzed a mutant strain that lacks a key component of the flagellar basal
238 body, FliM, and is aflagellated (41). SEM analysis of the Δ*fliM* mutant showed a complete loss
239 of flagella (Fig. 7A). This mutant displayed significantly less biofilm biomass (Fig. 7B), but we
240 were able to find few microcolonies. Within these microcolonies, the filaments were completely
241 lacking (Fig. 7A). These results suggest that these filaments are flagella, and furthermore that
242 flagella and/or motility are important for biofilm formation.

243 To further dissect the roles of motility and flagella in biofilm formation, we analyzed
244 biofilm formation in a non-motile but flagellated strain created by disruption of the motor protein
245 MotB. As reported previously, this mutant still expresses flagella (Fig. 7A). Biofilm formation,
246 however, was severely impaired compared to the wild-type strain, which suggest that a lack of
247 motility might contribute to the biofilm defect. However, Δ*motB* produced significantly more
248 biofilm than Δ*fliM* mutant suggesting that the flagella structure even in absence of motility also
249 contributes to biofilm formation in *H. pylori*.

250 To examine whether other strains of *H. pylori* similarly use flagella in biofilms, we
251 imaged the biofilm of *H. pylori* strain G27 and similar flagellar mutants as used above. Wild-

252 type *H. pylori* G27 biofilm cells also contained filaments consistent with flagella (Fig. 8A). As
253 with strain SS1, mutants lacking flagella (*flgS or fliA*) formed very weak biofilms, while strains
254 that had flagella but no motility (*motB*) retained partial biofilm formation (Fig. 8B).
255 Taken together, these data suggest that flagella are produced by *H. pylori* when in a
256 biofilm, and appear to play roles in addition to simple motility, promoting biofilm integrity by
257 holding cells together and to the surface,
258

DISCUSSION

In this report, we present the first transcriptomics characterization of the *H. pylori* biofilm. This study demonstrated clearly distinct expression profiles between planktonic and biofilm cells. The biofilm cells were characterized by low metabolic activity and triggering of several stress responses. Among the upregulated genes in the biofilm cells, we found several genes associated with cell membrane proteins, outer membrane proteins, stress response, and surprisingly, genes related to the flagellar apparatus. SEM analysis confirmed that flagella are present in a mature *H. pylori* biofilm, and appear to play a role in maintaining solid biofilm structures. This result was somewhat surprising, as typically flagella are proposed to be turned off during the sessile biofilm growth mode (42-44). Recent work however, discussed below, has suggested that flagella in *E. coli* biofilms may play a structural role. Our studies with *H. pylori* thus build on an emerging theme that flagella are not always turned off in mature biofilms, and indeed may play important functions in biofilm structure

To gain insights into the mechanisms behind the biofilm formation in *H. pylori*, we used RNA sequencing and carried out a comparative transcriptomic analysis between biofilm cells and those in the planktonic state. Using this approach, we observed that 8.18% of genes were significantly differentially expressed between biofilm and planktonic cells, similar to that reported in other bacterial systems (43, 45, 46). In our experimental design, we compared a static biofilm mode of growth, where attached cells adhered to the bottom of the wells, with planktonic non-attached cells in the same wells. This approach was used to maintain the same growth conditions as much as possible between biofilm and planktonic samples, and likely contributed to the relatively small number of differentially expressed genes. However, since biofilm formation is a dynamic process with frequent switching between planktonic to biofilm modes

283 occurring frequently, we likely have some contamination between the biofilm and planktonic
284 populations. Therefore, our method may have missed some genes that are expressed in either
285 population.

286 One of the findings from our transcriptomic analysis was that several flagellar protein
287 transcripts were significantly elevated in the biofilm. Notably, these were not for the entire
288 flagellum, but instead specific genes encoding the rod, hook, and filament. Specifically, we saw
289 biofilm-cell overexpression of genes encoding for the FlgB rod protein, the FlgE flagellar hook
290 protein, the FlgK and FlgL hook-filament junction proteins, the FliK hook length control protein
291 and two flagellins (FlaB and the putative flagellin encoded by FlaG). Notably absent was the
292 gene for the major flagellin FlaA, and genes for the motor and stator. We also saw the up-
293 regulation of *flgM* which encodes an anti-sigma factor that interacts with flagellar sigma factor
294 FliA, and therefore would be expected to decreased expression of *flaA* (47).

295 Historically, flagella have been typically viewed as important only for initial biofilm
296 attachment and later cell dispersion (44, 48). In fact, it has often been suggested that genes
297 encoding for flagella are turned off in mature biofilms (42-44). However, other reports have
298 shown that some microbes express flagella during all stages of biofilm development and not only
299 during the attachment and dispersion processes (49, 50). In *E. coli*, several flagellar-biosynthesis
300 genes were induced in mature biofilms, and around 20 flagellar genes were regulated throughout
301 all stages of biofilm development and not simply turned off (49). *E. coli* flagella were proposed
302 to have a structural role along with other matrix components (i.e. eDNA and extracellular
303 proteins), acting to cement and hold cells together and to the surface (50, 51). Our data
304 furthermore showed that aflagellated mutants are poor biofilm formers, supporting that these
305 filaments could play a structural role. Taken together, these findings suggest that flagella of *H.*

306 *pylori* may play a structural role during biofilm formation to help bacteria attach to each other
307 and to surfaces.

308 Interestingly, we found that the HspR and HrcA transcriptional repressor proteins are up-
309 regulated in biofilm cells. These proteins had previously been shown to positively correlate with
310 flagella expression (52), providing candidate regulatory proteins that function in biofilm cells.
311 HspR and HrcA belong to the heat shock protein family, and have been shown to respond to heat
312 shock temperature conditions although the nature of their "true" signal is not yet clear (52, 53). A
313 previous comparative transcriptomic analysis of wild-type *H. pylori* along with Δ*hspR*, Δ*hrcA*,
314 and double mutants revealed a set of 14 genes that were negatively regulated and 29 genes that
315 were positively regulated by these transcriptional regulators (52). The regulated genes include
316 those for chaperones, urease enzyme activity, adhesion to epithelial cells and flagella.
317 Interestingly, among the 29 positively regulated genes, nearly half (14) encoded for flagellar
318 genes, including the *flgM*, *flaG*, *fliD*, *flgK*, *flgB*, *flgE* and *fliK* transcripts we identified here.
319 Thus, our data suggest that biofilm conditions activate expression of HrcA and HspR, which in
320 turn upregulate a subset of flagellar genes.

321 Experiments suggest that HrcA and HspR regulators do not directly regulate the flagellar
322 genes (52). However, they do directly repress expression from several promoters including those
323 upstream of the *groESL*, *hrcA-grpE-dnaK*, and *cbpA-hspR-hp1026* operons. These gene products
324 encode the major chaperones of *H. pylori* (52-54). Heat shock conditions relieve the repression,
325 and allow expression of these operons. Consistent with elevated expression of HspR and HrcA,
326 we found the genes coding for the heat shock protein GroEL to be downregulated in biofilm. Our
327 data suggest that some yet-to-be determined conditions occurring during biofilm formation
328 trigger the expression of HspR and HcrA regulators.

Other genes associated with stress responses were also up-regulated in biofilm cells including the *pgdA* and *recR* genes. These genes encode for a peptidoglycan deacetylase and DNA recombination protein, respectively. RecR has been shown to be involved in repairing in DNA double strand breaks induced by oxidative stress (55) and the *recR* mutant was highly sensitive to DNA damaging agents, oxidative stress and had a reduced ability to colonize mouse stomachs (55). *pgdA* has been reported to be highly induced by oxidative stress (33, 56). Up-regulation of oxidative stress genes has previously been reported in biofilm cells of other organisms including *E. coli* (57), *Pseudomonas aeruginosa* (42), *Neisseria gonorrhoeae* (58) and *Clostridium perfringens* (48).

As reported for other microorganisms, *H. pylori* biofilm cells have altered metabolism, typically thought to be associated with the restricted availability of nutrients (48, 59). *H. pylori* biofilm cells were characterized by a downregulation of the expression of multiple genes involved in metabolism and translation including, *atpC*, *atpE*, *nifU* and several ribosomal protein genes. This low metabolism phenotype seems not be related simply to the presence of coccoid cells, but rather to the microenvironment generated during biofilm formation since the proportion of rods and coccoid forms did not differ between planktonic and biofilm populations.

H. pylori biofilm cells may also actively block the translational machinery, as suggested by the up-regulation of the gene encoding RsfS, a ribosomal silencing factor. This protein was previously described in *E. coli* and *Mycobacterium tuberculosis* to slow or block the translation machinery during stationary phase and/or nutrition-deficiency stress (60). It interacts with the 50S large ribosomal subunit, prevents its association with the 30 S ribosomal submit, and thus blocks formation of functional ribosomes (60). Whether it functions similarly in *H. pylori* remains to be determined.

These observations that biofilm cells may have decreased translation are relevant because at least two of the main antibiotics used to treat *H. pylori* infection, clarithromycin and tetracycline, inhibit the 50S and 30S ribosomal subunits, respectively. Thus, these antibiotics may have less impact on biofilm cells. In fact, recent *in vitro* studies have shown that clarithromycin is 4 to 16-fold less effective on *H. pylori* biofilm cells as compared to planktonic ones (26, 61).

Taken together, our study has shown that *H. pylori* biofilm cells display a distinct transcriptomic profile compared to their planktonic counterparts. Lower metabolism and stress responses, likely associated to the microenvironment generated in the *H. pylori* biofilm, could be determinants of antimicrobial tolerance and involved in the persistence and survival of *H. pylori*. However, the up-regulated and down-regulated genes identified in this study are not specific for biofilm cells, and stress response genes have been previously observed in other conditions when both planktonic or biofilm cells were exposed to various stresses. Therefore, our data do not support the existence of a biofilm-specific genetic program. Additionally, our data show that flagella filaments are upregulated in biofilm cells and form an integral part of the biofilm matrix. Indeed, *H. pylori* without flagella form weak biofilms. These results thus contribute to correcting the idea that flagella are only involved during the first and last steps of biofilm formation, and instead support their importance throughout the biofilm process.

MATERIALS AND METHODS

Bacterial strain and growth conditions. *H. pylori* Sydney strain 1 (SS1) (62) and all other *H. pylori* strains used in this study are listed in Table.1. Strains were grown on Columbia Horse Blood Agar (CHBA), containing: 0.2%-β-cyclodextrin, 10μg/ml vancomycin, 5μg/ml of cefsulodin, 2.5 U/ml polymyxin B, 5μg/ml trimethoprim, and 8μg/ml amphotericin B (all chemicals from Thermo Fisher or Gold Biotech). Cultures were grown under micro-aerobic conditions (5% O_2 and 10% CO_2) at 37°C. For liquid culture and biofilm assay, *H. pylori* was grown in Brucella broth (Difco) containing 10% heat inactivated fetal bovine serum (FBS) (BB10; Gibco/BRL) with constant shaking under microaerobic conditions. For biofilm formation, several conditions were tested including Brucella broth containing different percentage of FBS (BB2, BB6 and BB10), and HAM's F-12 (PAA Laboratories GmbH, Pasching, Austria) containing 10% or 2% of FBS (HAMS10 and HAMS2).

Biofilm assays. Biofilm formation assays were carried as described previously, with slight modification (27). *H. pylori* SS1 was grown overnight in BB10 as above, diluted to and OD600 of 0.15 with fresh BB10, BB2, BB6 or HAMS media as desired, and then used to fill triplicate wells of a sterile 96-well polystyrene microtiter plate (Costar, 3596). Following static incubation of 1, 2, 3 or 5 days under micro aerobic conditions, culture medium was removed by aspiration and the plate was washed twice using PBS. The wells were then filled with 200μL of crystal violet (0.1 % wt/vol), and the plate was incubated for 2 min at room temperature. After removal of the crystal violet solution by aspiration, the plate was washed twice with PBS and dried for 20

min at room temperature. To visualize biofilms, 200 µL of ethanol (70% vol/vol) was added to the wells and the absorbance at 590 nm was measured.

Biofilm dispersion assays. To evaluated the composition of SS1 biofilm matrix, we assessed the response of preformed biofilms to different enzymatic treatment. DNAse I and proteinase K (both from Sigma-Aldrich) were used to target, extracellular DNA and extracellular proteins, respectively. Biofilms were grown as described above and after three-days of growth, the old media were replaced by fresh media containing different concentrations of DNase I (380µg/ml to 95µg/ml) or proteinase K (200ug/ml to 50 ug/ml). The cells were then incubated for a further 24 hours. Control wells were exposed to media without enzyme. After treatments, the biofilm was stained with crystal violet as described above. Results are presented a percentage of the untreated control.

Confocal laser scanning microscopy. Biofilms of *H. pylori* SS1 were prepared as described above using BB2, however, for confocal laser scanning microscopy (CLSM), µ-Slide 8-well glass bottom chamber slides (ibidi, Germany) were used instead of 96-well microtiter plates. Three day-old biofilms were stained with FilmTracer™ FM®1–43 (Invitrogen), BOBO-3 (Invitrogen), Filmtracer SYPRO Ruby biofilm matrix stain (Invitrogen), or FilmTracer LIVE/DEAD biofilm viability kit (Invitrogen) according to the manufacture's instructions. Stained biofilms were visualized by CLSM with an LSM 5 Pascal laser-scanning microscope (Zeiss) and images were acquired using Imaris software (Bitplane). Biomass analysis of biofilm was carried using FM®1–43 stained z-stack images (0.1µm thickness) obtained by CLSM from randomly selected areas. The biomass of biofilms was determined using COMSTAT (63).

RNA extraction and library construction. Biofilms of *H. pylori* SS1 were grown in 6-well plates (Costar) in BB2 as above. After 3 days of incubation, media containing non-attached planktonic bacteria (the planktonic fraction) was removed by pipetting, the cells were harvested by centrifugation and washed twice with PBS. The attached bacteria, representing the biofilm fraction, were washed twice with PBS to remove any remaining planktonic cells. Attached cells were scrapped off the plate using cell scraper. Both planktonic and biofilm fractions were subject to total RNA extraction using Trizol Max bacterial enhancement kit (Ambion, Life Technology, Carlsbad, CA, USA) as described by the manufacturer. RNA was further purified and concentrated using an RNAeasy Kit (Qiagen). rRNA was removed using the RiboZero magnetic kit (Illumina). Sequencing libraries were generated using NEBNext Ultra^{TM} Directional RNA library Prep Kit for Illumina (NEB, USA). cDNA library quality and amount was verified using Agilent Bioanalyzer 2100 system (Agilent technologies, CA, USA) and then sequenced using Illumina NextSeq Mid-Output (UC Davis Genome Center).

Transcriptomic analysis. RNA-seq data were analyzed using CLC Genomics Workbench (Version 11.0, CLC Bio, Boston, MA, USA). After adapters were trimmed, forward and reverse sequenced reads generated for each growth state (biofilm vs planktonic; three biological replicates for each condition) were mapped against the SS1 reference genome (32) to quantify gene expression levels for each experimental condition. The expression value was measured in Reads per Kilobase Per Million Mapped Reads (RPKM). Genes were considered as differentially expressed when the log2 (fold change) was above 1 and the *P*-value was lower than 0.05.

438 ***Quantitative PCR.*** To validate the RNA-seq data, we performed qPCR to quantify the
439 transcription of four differentially expressed genes (two up-regulated genes and two down-
440 regulated genes). The Fold change in gene expression was calculated after normalization of each
441 gene with the constitutively expressed gene *gapB* (64). Primers used for this experiment are
442 listed 5'-3' below: gapB forward: GCCTCTTGCACGACTAACGC; gapB reverse:
443 CTTTGCTCACGCCGGTGCTT. flgL forward: CAGGCAGCTCATGGATGCGA; flgL reverse:
444 CGCTGTGCAAGGCGTTTTGA; hspR forward: TAGGCGTGCACCCTCAAACC; hspR
445 reverse: CGCCCGCTAGATTAACCCCC; hcpC forward: GGGTTTTGTGCTTGGGTGCG;
446 hcpC reverse: TTCCACCCCCTGCCCTTGAT; hslV forward:
447 GATTTGCCGGAAGCACTGCG; hslV reverse: ATCATCGCTTCCAGTCGGCG

448
449 ***Construction of H. pylori mutants.***

450 The SS1 Δ*fliM* mutant was created by natural transformation of SS1 wild type with plasmid
451 pBS-fliM::catmut (40) which replaces most of the fliM gene, corresponding to amino acids 1-
452 105, with cat. The G27 *motB* mutant was created by natural transformation of G27 wild type
453 with plasmid pKO114K and selection for kanamycin resistance. pKO114K was made as
454 described for pKO114i (65), but instead of insertion of a aphA3-sacB allele, only an aphA3
455 allele was inserted. This allele inserts the aphA3 at the position corresponding to amino acid 113
456 of 257.

457 ***Scanning electron microscopy.*** *H. pylori* biofilms were grown on glass coverslips (12mm,
458 Chemgalss, life Sciences, Vineland, NJ) by dispersing 4 mL of a culture diluted to OD 0.15 in
459 BB2 into wells of a 6-well plate (Costar). The plate was incubated as described above. After
460 three days of growth, biofilms formed on the surface of the coverslips and planktonic cells were
461 washed twice with PBS and fixed with 2.5% glutaraldehyde (wt/vol) for 1 hour at room

462 temperature. Samples were then dehydrated with graded ethanol series, critically point dried,
463 sputtered with ~20 nm of gold (Hammer IV, Technics Inc, Anaheim, CA) and imaged in
464 an FEI Quanta 3D Dualbeam SEM operating at 5 kV and 6.7 pA.
465
466 ***Statistical analysis.*** Biofilms data were analyzed with GraphPad Prism (version 7.0) software
467 (GraphPad Inc., San Diego, CA) using one-way analysis of variance (ANOVA) followed by
468 Dunnett's multiple-comparison test.
469

ACKNOWLEDGEMENTS

We thank Dr. Fitnat Yildiz (U.C. Santa Cruz) and Dr. Davide Roncarati (University of Bologna, Italy) for their helpful suggestions and comments on the study and the manuscript. We thank Aaron Clarke (U.C. Santa Cruz) for his assistance with portions of the SEM experiments. We thank Dr. Ben Abrams (U.C. Santa Cruz) for CLSM assistance. We also acknowledge Dr. Tom Yuzvinsky (U.C. Santa Cruz) for assistance with sample preparation and electron microscopy and the W.M. Keck Center for Nanoscale Optofluidics for use of the FEI Quanta 3D Dualbeam microscope. We also thank Dr. David Bernick and METX department (U.C. Santa Cruz) for holding and financially supporting the RNAseq workshop. The work described here was supported by National Institutes of Health National Institute of Allergy and Infectious Disease (NIAID) grant RO1AI116946 (to K.M.O.). The funders had no role in study design, data collection and interpretation, or the decision to submit the work for publication.

485 **FIGURES LEGENDS**

486

487 **FIG 1. *H. pylori* SS1 forms robust biofilms after 3 days of growth in BB2.** *H. pylori* strain
488 SS1 was grown in the indicated media and biofilm formation was assessed by crystal violet
489 absorbance at 595nm. **(A)** *H. pylori* SS1 was grown for 3 days in BB media supplemented with
490 different concentration of FBS (BB10: 10%, BB6: 6% and BB2: 2%). **(B)** *H. pylori* SS1 was
491 grown for 3 days in BB media or HAMS F12 supplemented with 10% or 2% of FBS. **(C)** *H.*
492 *pylori* SS1 was grown in BB media supplemented with 2% FBS and biofilm formation was
493 evaluated at different time points. Experiments were performed three independent times with at
494 least 6 technical replicates for each. Statistical analysis was performed using ANOVA (*, $P <$
495 0.05 and **, $P < 0.01$).

496

497 **FIG 2. Confocal scanning laser microscopy (CSLM) images of *H. pylori* SS1 biofilm.** Shown
498 are representative CSLM images of 3 day-old SS1 biofilms grown in BB2 and stained with **(A)**
499 FM 1-43 to stain total bacterial cells; **(B)** SYPRO RUBY to stain extracellular proteins, **(C)**
500 BOBO-3 to stain extracellular DNA and **(D-F)** Live-Dead staining with live cells represented by
501 the green-fluorescent SYTO 9, and dead/damaged cells by the red-fluorescent propidium. Scale
502 bar = 30 µm

503

504 **FIG 3. Effect of enzymatic treatments on pre-formed biofilms.** *H. pylori* SS1 was allowed to
505 form biofilms for three days in BB2. The media was then removed and replaced with either fresh
506 media or media containing DNase I or proteinase K. Cells were re-incubated for 24 hours, and
507 then analyzed for remaining biofilm using the crystal violet assay. Data shown here represent the
508 percentage of remaining of biofilm compared to the untreated control. Experiments were

509 performed three times independently with at least 8 technical replicates for each. Statistical
510 analysis was performed using ANOVA *, $P < 0.01$ compared to the untreated control.
511
512 **FIG 4. Biofilm-grown cells and planktonic cells show distinct transcriptional profiles. (A)**
513 principal component analysis (PCA) of gene expression obtained by RNA-seq between biofilm
514 (n =3) and planktonic (n =3) populations. **(B)** Volcano plot of gene expression data. The y-axis is
515 the negative log10 of P-values (a higher value indicates greater significance) and the x-axis is
516 log2 fold change in difference in abundance between two population (positive values represent
517 the up-regulated genes in biofilm and negative values represent down-regulated genes). The
518 dashed red line shows where P =0.01, with points above the line having $P < 0.01$ and points
519 below the line having $P > 0.01$.
520
521 **FIG 5. Functional classification of genes differentially expression in *H. pylori* SS1 biofilm.**
522 Black and grey bars represent up-regulated and down-regulated genes, respectively that were
523 significantly differentially expressed ($p< 0.01$ and $\log_2$-fold change >1 or <-1) between *H. pylori*
524 biofilm and planktonic populations
525
526 **FIG 6. qPCR validation of the transcription of selected differentially expressed genes.** The
527 data indicate the fold-change expression of genes in *H. pylori* biofilm cells compared to
528 planktonic cells. Fold-change in gene expressions were calculated after normalization of each
529 gene with the constitutively expressed gene control *gapB*. Bars represent the mean and the error
530 bars the standard error of the mean, Black and grey bars represent qPCR and RNA-seq results,

531 respectively. Statistical analyses were performed using $2^{-\Delta\Delta}CT$ values, and all results with an
532 asterisk were statistically significant ($P < 0.01$).
533
534 **FIG 7. Flagella play integral roles in *H. pylori* biofilms. (A)** Scanning electron microscope
535 (SEM) images of biofilms formed by *H. pylori* wild-type SS1 (SS1 WT), isogenic non-motile but
536 flagellated mutant Δ*motB* (SS1 Δ*motB*), and isogenic aflagellated mutant Δ*fliM* (SS1 Δ*fliM*).
537 Arrows flagella. **(B)** Quantification of biofilm formation by *H. pylori* SS1 WT, Δ*motB* and
538 Δ*fliM*. Strains were grown in BB2 media for three days, followed by biofilm evaluation using the
539 crystal violet assay. Experiments were performed three times independently with 6-9 technical
540 replicates for each. Statistical analysis was performed using ANOVA (**, $P < 0.01$ and *, $P <$
541 0.05).
542
543 **Fig 8. *H. pylori* G27 biofilm contain structurally important flagella. (A)** Scanning electron
544 microscope (SEM) images of wild type G27 *H. pylori* biofilms. Arrows indicate flagella. **(B)**
545 Quantification of biofilm formation by *H. pylori* G27 wild type (WT), non-motile flagellated
546 *motB,* non-motile mutant *fliA* that is reported to have either truncated flagella or no flagella, and
547 the aflagellated and non-motile mutant *flgS***.** Biofilms were evaluated using the crystal violet
548 assay. Experiments were performed 2 times independently with at least 6 technical replicates for
549 each. Statistical analysis was performed using ANOVA (**, $P < 0.01$ and *, $P < 0.05$).
550
551 **Supplementary Movie 1. Three-dimensional (3D) view of *H. pylori* biofilm grown for 3**
552 **days.** Bacteria were stained with FilmTracer™ FM®1–43 and observed by CLSM.

553 **REFERENCES**

554 1. **Moodley Y, Linz B, Bond RP, Nieuwoudt M, Soodyall H, Schlebusch CM, Bernhoft**
555 **S, Hale J, Suerbaum S, Mugisha L, van der Merwe SW, Achtman M.** 2012. Age of
556 the association between *Helicobacter pylori* and man. PLoS Pathog **8:**e1002693.
557 2. **Salama NR, Hartung ML, Muller A.** 2013. Life in the human stomach: persistence
558 strategies of the bacterial pathogen *Helicobacter pylori*. Nat Rev Microbiol **11:**385-399.
559 3. **Schreiber S, Konradt M, Groll C, Scheid P, Hanauer G, Werling HO, Josenhans C,**
560 **Suerbaum S.** 2004. The spatial orientation of *Helicobacter pylori* in the gastric mucus.
561 Proc Natl Acad Sci U S A **101:**5024-5029.
562 4. **Keilberg D, Zavros Y, Shepherd B, Salama NR, Ottemann KM.** 2016. Spatial and
563 temporal shifts in bacterial biogeography and gland occupation during the development
564 of a chronic infection. MBio **7**.
565 5. **Howitt MR, Lee JY, Lertsethtakarn P, Vogelmann R, Joubert LM, Ottemann KM,**
566 **Amieva MR.** 2011. ChePep controls *Helicobacter pylori* infection of the gastric glands
567 and chemotaxis in the Epsilonproteobacteria. MBio **2**.
568 6. **Hu Q, Zhang Y, Zhang X, Fu K.** 2016. Gastric mucosa-associated lymphoid tissue
569 lymphoma and *Helicobacter pylori* infection: a review of current diagnosis and
570 management. Biomark Res **4:**15.
571 7. **Kim SY, Choi DJ, Chung JW.** 2015. Antibiotic treatment for *Helicobacter pylori*: Is the
572 end coming? World J Gastrointest Pharmacol Ther **6:**183-198.
573 8. **Parkin DM.** 2006. The global health burden of infection-associated cancers in the year
574 2002. Int J Cancer **118:**3030-3044.
575 9. **Choi IJ, Kook MC, Kim YI, Cho SJ, Lee JY, Kim CG, Park B, Nam BH.** 2018.
576 *Helicobacter pylori* therapy for the prevention of metachronous gastric Cancer. N Engl J
577 Med **378:**1085-1095.
578 10. **Keilberg D, Ottemann KM.** 2016. How *Helicobacter pylori* senses, targets and interacts
579 with the gastric epithelium. Environ Microbiol **18:**791-806.
580 11. **Celli JP, Turner BS, Afdhal NH, Keates S, Ghiran I, Kelly CP, Ewoldt RH,**
581 **McKinley GH, So P, Erramilli S, Bansil R.** 2009. *Helicobacter pylori* moves through
582 mucus by reducing mucin viscoelasticity. Proc Natl Acad Sci U S A **106:**14321-14326.

12. **Tan S, Tompkins LS, Amieva MR.** 2009. *Helicobacter pylori* usurps cell polarity to turn the cell surface into a replicative niche. PLoS Pathog **5:**e1000407.
13. **Anderson JK, Huang JY, Wreden C, Sweeney EG, Goers J, Remington SJ, Guillemin K.** 2015. Chemorepulsion from the quorum signal autoinducer-2 promotes *Helicobacter pylori* biofilm dispersal. MBio **6:**e00379.
14. **Flemming HC, Wingender J.** 2010. The biofilm matrix. Nat Rev Microbiol **8:**623-633.
15. **Hathroubi S, Mekni MA, Domenico P, Nguyen D, Jacques M.** 2017. Biofilms: Microbial shelters against antibiotics. Microb Drug Resist **23:**147-156.
16. **Sapi E, Balasubramanian K, Poruri A, Maghsoudlou JS, Socarras KM, Timmaraju AV, Filush KR, Gupta K, Shaikh S, Theophilus PA, Luecke DF, MacDonald A, Zelger B.** 2016. Evidence of *in Vivo* existence of Borrelia biofilm in Borrelial lymphocytomas. Eur J Microbiol Immunol (Bp) **6:**9-24.
17. **Boisvert AA, Cheng MP, Sheppard DC, Nguyen D.** 2016. Microbial biofilms in pulmonary and critical care diseases. Ann Am Thorac Soc **13:**1615-1623.
18. **Hall-Stoodley L, Hu FZ, Gieseke A, Nistico L, Nguyen D, Hayes J, Forbes M, Greenberg DP, Dice B, Burrows A, Wackym PA, Stoodley P, Post JC, Ehrlich GD, Kerschner JE.** 2006. Direct detection of bacterial biofilms on the middle-ear mucosa of children with chronic otitis media. JAMA **296:**202-211.
19. **Vakil N, Vaira D.** 2013. Treatment for *H. pylori* infection: new challenges with antimicrobial resistance. J Clin Gastroenterol **47:**383-388.
20. **Hathroubi S, Servetas SL, Windham I, Merrell DS, Ottemann KM.** 2018. *Helicobacter pylori* biofilm formation and its potential role in pathogenesis. Microbiol Mol Biol Rev **82**.
21. **Carron MA, Tran VR, Sugawa C, Coticchia JM.** 2006. Identification of *Helicobacter pylori* biofilms in human gastric mucosa. J Gastrointest Surg **10:**712-717.
22. **Coticchia JM, Sugawa C, Tran VR, Gurrola J, Kowalski E, Carron MA.** 2006. Presence and density of *Helicobacter pylori* biofilms in human gastric mucosa in patients with peptic ulcer disease. J Gastrointest Surg **10:**883-889.
23. **Cole SP, Harwood J, Lee R, She R, Guiney DG.** 2004. Characterization of monospecies biofilm formation by *Helicobacter pylori*. J Bacteriol **186:**3124-3132.

24. **Windham IH, Servetas SL, Whitmire JM, Pletzer D, Hancock REW, Merrell DS.** 2018. *Helicobacter pylori* biofilm formation is differentially affected by common Culture conditions, and proteins play a central role in the biofilm Matrix. Appl Environ Microbiol **84**.

25. **Yang FL, Hassanbhai AM, Chen HY, Huang ZY, Lin TL, Wu SH, Ho B.** 2011. Proteomannans in biofilm of *Helicobacter pylori* ATCC 43504. Helicobacter **16:**89-98.

26. **Yonezawa H, Osaki T, Hanawa T, Kurata S, Ochiai K, Kamiya S.** 2013. Impact of *Helicobacter pylori* biofilm formation on clarithromycin susceptibility and generation of resistance mutations. PLoS One **8:**e73301.

27. **Bessa LJ, Grande R, Di Iorio D, Di Giulio M, Di Campli E, Cellini L.** 2013. *Helicobacter pylori* free-living and biofilm modes of growth: behavior in response to different culture media. APMIS **121:**549-560.

28. **Williams JC, McInnis KA, Testerman TL.** 2008. Adherence of *Helicobacter pylori* to abiotic surfaces is influenced by serum. Appl Environ Microbiol **74:**1255-1258.

29. **Hathroubi S, Hancock MA, Bosse JT, Langford PR, Tremblay YD, Labrie J, Jacques M.** 2015. Surface polysaccharide mutants reveal that absence of O antigen reduces biofilm formation of *Actinobacillus pleuropneumoniae*. Infect Immun **84:**127-137.

30. **Vogeleer P, Tremblay YDN, Jubelin G, Jacques M, Harel J.** 2015. Biofilm-forming abilities of shiga toxin-producing *Escherichia coli* isolates associated with human infections. Appl Environ Microbiol **82:**1448-1458.

31. **Grande R, Di Giulio M, Bessa LJ, Di Campli E, Baffoni M, Guarnieri S, Cellini L.** 2011. Extracellular DNA in *Helicobacter pylori* biofilm: a backstairs rumour. J Appl Microbiol **110:**490-498.

32. **Draper JL, Hansen LM, Bernick DL, Abedrabbo S, Underwood JG, Kong N, Huang BC, Weis AM, Weimer BC, van Vliet AH, Pourmand N, Solnick JV, Karplus K, Ottemann KM.** 2017. Fallacy of the unique genome: Sequence diversity within single *Helicobacter pylori* strains. MBio **8**.

33. **Wang G, Maier RJ.** 2015. A novel DNA-binding protein plays an important role in *Helicobacter pylori* stress tolerance and survival in the host. J Bacteriol **197:**973-982.

643 34. **Hong SH, Lee J, Wood TK.** 2010. Engineering global regulator Hha of *Escherichia coli*
644 to control biofilm dispersal. Microb Biotechnol **3:**717-728.
645 35. **Formichella L, Romberg L, Bolz C, Vieth M, Geppert M, Gottner G, Nolting C,**
646 **Walter D, Schepp W, Schneider A, Ulm K, Wolf P, Busch DH, Soutschek E,**
647 **Gerhard M.** 2013. A novel line immunoassay based on recombinant virulence factors
648 enables highly specific and sensitive serologic diagnosis of *Helicobacter pylori* infection.
649 Clin Vaccine Immunol **20:**1703-1710.
650 36. **Zhao Y, Yokota K, Ayada K, Yamamoto Y, Okada T, Shen L, Oguma K.** 2007.
651 *Helicobacter pylori* heat-shock protein 60 induces interleukin-8 via a Toll-like receptor
652 (TLR)2 and mitogen-activated protein (MAP) kinase pathway in human monocytes. J
653 Med Microbiol **56:**154-164.
654 37. **Kusters JG, van Vliet AH, Kuipers EJ.** 2006. Pathogenesis of *Helicobacter pylori*
655 infection. Clin Microbiol Rev **19:**449-490.
656 38. **Ta LH, Hansen LM, Sause WE, Shiva O, Millstein A, Ottemann KM, Castillo AR,**
657 **Solnick JV**. 2012. Conserved transcriptional unit organization of the cag pathogenicity
658 island among *Helicobacter pylori* strains. Front Cell Inf Microbio **2**, 46
659 39. **Backert S, Tegtmeyer N, Fischer W.** 2015. Composition, structure and function of the
660 Helicobacter pylori cag pathogenicity island encoded type IV secretion system. Future
661 Microbiol **10**, 955–965.
662 40. **O'Rourke J, Bode G.** 2001. Morphology and ultrastructure. *In* Mobley HLT, Mendz GL,
663 Hazell SL (ed), *Helicobacter pylori*: Physiology and genetics, Washington (DC).
664 41. **Lowenthal AC, Hill M, Sycuro LK, Mehmood K, Salama NR, Ottemann KM.** 2009.
665 Functional analysis of the *Helicobacter pylori* flagellar switch proteins. J Bacteriol
666 **191:**7147-7156.
667 42. **Sauer K, Camper AK, Ehrlich GD, Costerton JW, Davies DG.** 2002. *Pseudomonas*
668 *aeruginosa* displays multiple phenotypes during development as a biofilm. J Bacteriol
669 **184:**1140-1154.
670 43. **Whiteley M, Bangera MG, Bumgarner RE, Parsek MR, Teitzel GM, Lory S,**
671 **Greenberg EP.** 2001. Gene expression in *Pseudomonas aeruginosa* biofilms. Nature
672 **413:**860-864.

673 44. **Guttenplan SB, Kearns DB.** 2013. Regulation of flagellar motility during biofilm
674 formation. FEMS Microbiol Rev **37:**849-871.
675 45. **Romero-Lastra P, Sanchez MC, Ribeiro-Vidal H, Llama-Palacios A, Figuero E,**
676 **Herrera D, Sanz M.** 2017. Comparative gene expression analysis of *Porphyromonas*
677 *gingivalis* ATCC 33277 in planktonic and biofilms states. PLoS One **12:**e0174669.
678 46. **Beloin C, Valle J, Latour-Lambert P, Faure P, Kzreminski M, Balestrino D,**
679 **Haagensen JA, Molin S, Prensier G, Arbeille B, Ghigo JM.** 2004. Global impact of
680 mature biofilm lifestyle on *Escherichia coli* K-12 gene expression. Mol Microbiol
681 **51:**659-674.
682 47. **Josenhans C, Niehus E, Amersbach S, Horster A, Betz C, Drescher B, Hughes KT,**
683 **Suerbaum S.** 2002. Functional characterization of the antagonistic flagellar late
684 regulators FliA and FlgM of *Helicobacter pylori* and their effects on the *H. pylori*
685 transcriptome. Mol Microbiol **43:**307-322.
686 48. **Charlebois A, Jacques M, Archambault M.** 2016. Comparative transcriptomic analysis
687 of *Clostridium perfringens* biofilms and planktonic cells. Avian Pathol **45:**593-601.
688 49. **Domka J, Lee J, Bansal T, Wood TK.** 2007. Temporal gene-expression in *Escherichia*
689 *coli* K-12 biofilms. Environ Microbiol **9:**332-346.
690 50. **Serra DO, Richter AM, Klauck G, Mika F, Hengge R.** 2013. Microanatomy at cellular
691 resolution and spatial order of physiological differentiation in a bacterial biofilm. MBio
692 **4:**e00103-00113.
693 51. **Hung C, Zhou Y, Pinkner JS, Dodson KW, Crowley JR, Heuser J, Chapman MR,**
694 **Hadjifrangiskou M, Henderson JP, Hultgren SJ.** 2013. *Escherichia coli* biofilms have
695 an organized and complex extracellular matrix structure. MBio **4:**e00645-00613.
696 52. **Roncarati D, Danielli A, Spohn G, Delany I, Scarlato V.** 2007. Transcriptional
697 regulation of stress response and motility functions in *Helicobacter pylori* is mediated by
698 HspR and HrcA. J Bacteriol **189:**7234-7243.
699 53. **Spohn G, Scarlato V.** 1999. The autoregulatory HspR repressor protein governs
700 chaperone gene transcription in *Helicobacter pylori*. Mol Microbiol **34:**663-674.
701 54. **Spohn G, Danielli A, Roncarati D, Delany I, Rappuoli R, Scarlato V.** 2004. Dual
702 control of *Helicobacter pylori* heat shock gene transcription by HspR and HrcA. J
703 Bacteriol **186:**2956-2965.

55. **Wang G, Lo LF, Maier RJ.** 2011. The RecRO pathway of DNA recombinational repair in *Helicobacter pylori* and its role in bacterial survival in the host. DNA Repair (Amst) **10:**373-379.

56. **Wang G, Maier SE, Lo LF, Maier G, Dosi S, Maier RJ.** 2010. Peptidoglycan deacetylation in *Helicobacter pylori* contributes to bacterial survival by mitigating host immune responses. Infect Immun **78:**4660-4666.

57. **Schembri MA, Kjaergaard K, Klemm P.** 2003. Global gene expression in *Escherichia coli* biofilms. Mol Microbiol **48:**253-267.

58. **Falsetta ML, Steichen CT, McEwan AG, Cho C, Ketterer M, Shao J, Hunt J, Jennings MP, Apicella MA.** 2011. The Composition and Metabolic Phenotype of *Neisseria gonorrhoeae* Biofilms. Front Microbiol **2:**75.

59. **Castro J, Franca A, Bradwell KR, Serrano MG, Jefferson KK, Cerca N.** 2017. Comparative transcriptomic analysis of *Gardnerella vaginalis* biofilms vs. planktonic cultures using RNA-seq. NPJ Biofilms Microbiomes **3:**3.

60. **Hauser R, Pech M, Kijek J, Yamamoto H, Titz B, Naeve F, Tovchigrechko A, Yamamoto K, Szaflarski W, Takeuchi N, Stellberger T, Diefenbacher ME, Nierhaus KH, Uetz P.** 2012. RsfA (YbeB) proteins are conserved ribosomal silencing factors. PLoS Genet **8:**e1002815.

61. **Bugli F, Palmieri V, Torelli R, Papi M, De Spirito M, Cacaci M, Galgano S, Masucci L, Paroni Sterbini F, Vella A, Graffeo R, Posteraro B, Sanguinetti M.** 2016. *In vitro* effect of clarithromycin and alginate lyase against *Helicobacter pylori* biofilm. Biotechnol Prog **32:**1584-1591.

62. **Lee A, O'Rourke J, De Ungria MC, Robertson B, Daskalopoulos G, Dixon MF.** 1997. A standardized mouse model of *Helicobacter pylori* infection: introducing the Sydney strain. Gastroenterology **112:**1386-1397.

63. **Heydorn A, Nielsen AT, Hentzer M, Sternberg C, Givskov M, Ersboll BK, Molin S.** 2000. Quantification of biofilm structures by the novel computer program COMSTAT. Microbiol **146 (Pt 10):**2395-2407.

64. **Collins KD, Hu S, Grasberger H, Kao JY, Ottemann KM.** 2018. Chemotaxis allows bacteria to overcome host-generated reactive oxygen species that constrain gland colonization. Infect Immun doi:10.1128/IAI.00878-17.

65. **Ottemann KM, Lowenthal AC.** 2002. *Helicobacter pylori* uses motility for initial colonization and to attain robust infection. Infect Immun **70:**1984-1990.

66. **Censini S, Lange C, Xiang Z, Crabtree JE, Ghiara P, Borodovsky M, Rappuoli R, Covacci A.** 1996. cag, a pathogenicity island of *Helicobacter pylori*, encodes type I-specific and disease-associated virulence factors. Proc Natl Acad Sci U S A **93:**14648-14653.

67. **Salama NR, Shepherd B, Falkow S.** 2004. Global transposon mutagenesis and essential gene analysis of *Helicobacter pylori*. J Bacteriol **186:**7926-7935.

743 **Table 1. Strains used in this study.**
744

***H. pylori* strain**	**KO Strain number**	**Description/genotype**	**Reference/source**
SS1 WT		Wild-type strain	(62)/ J. O'Rourke
SS1 *ΔfliM*	KO1064	*ΔfliM::cat*	This study (allele published in (41))
SS1 *ΔmotB*	KO536	*ΔmotB2*	(65)
G27 WT		Wild-type strain	(66)/ N. Salama, Fred Hutchison Cancer Research Center, Seattle
G27 *motB*	KO493	*motB::aphA3*	This study
G27 *flgS*	KO688	*flgS::TnCat*	(67)
G27 *fliA*	KO689	*fliA::TnCat*	(67)

745

Table 2. Up-regulated gene in *H. pylori* SS1 biofilm (cutoff ratio ≥ 1 log2 fold change and p-value <0.05) using RNA-seq analysis, grouped by functional role categories. Fold change represents the difference in gene expression between biofilm (n =3) and planktonic (n =3) populations.

Locus Name	Putative identification	Fold Change
Cell envelope		
***flgL* (HPYLSS1_00284)**	Flagellar hook-associated protein 3	7.64
***flgK* (HPYLSS1_01062)**	flagellar hook-associated protein 1	6.16
***flgM* (HPYLSS1_01066)**	Anti-sigma-28 factor	3.94
***flaG* (HPYLSS1_00586)**	Polar flagellin G	3.93
***flaB* (HPYLSS1_00110)**	Flagellin B	3.52
***flgE1* (HPYLSS1_00464)**	Flagellar hook protein 1	3.07
***flgB* (HPYLSS1_01503)**	Flagellar basal body rod protein	2.37
***fliL* (HPYLSS1_00526)**	Flagellar protein of unknown function	2.25
***fliK* (HPYLSS1_00653)**	Flagellar hook-length control protein	2.14
***fliD* (HPYLSS1_00585)**	Flagellar hook-associated protein 2	2
***lpxB* (HPYLSS1_00467)**	Lipid-A-disaccharide synthase	3.06
***lptB* (HPYLSS1_00622)**	Lipopolysaccharide export system ATP-binding	2.54
***mltD* (HPYLSS1_01517)**	Membrane-bound lytic murein transglycosylase D precursor	2
***pgdA* (HPYLSS1_00299)**	Peptidoglycan deacetylase	2.1
HPYLSS1_00450	Membrane protein	3.78
HPYLSS1_01378	Outer membrane protein *homD*	3.26
HPYLSS1_01113	Putative outer membrane protein	2.91
HPYLSS1_01021	Outer membrane protein *homC*	2.69
HPYLSS1_01469	Putative outer membrane protein	2.52
Cellular process		

***cagE* (HPYLSS1_00705)**	Type IV secretion system protein virB4/DNA transfer	2.46
***cagW* (HPYLSS1_00718)**	CAG pathogenicity island protein CagW (cag10)	2.31
***cagL* (HPYLSS1_00710)**	CAG pathogenicity island protein CagL (cag18)	2.02
***recR* (HPYLSS1_00636)**	Recombination protein RecR	3.7
HPYLSS1_00410	DNA polymerase I	2.08
HPYLSS1_01332	CMP-N-acetylneuraminate-beta-galactosamide-	2.2
Regulatory functions		
***hrcA* (HPYLSS1_00106)**	Heat-inducible transcription repressor HrcA	4.84
***hspR* (HPYLSS1_00407)**	Putative heat shock protein HspR	2.09
***crdR* (HPYLSS1_01312)**	Two component response regulator CrdR	2.03
***rsfS* (HPYLSS1_01340)**	Ribosomal silencing factor S	2.16
Translation		
***ansA* (HPYLSS1_00615)**	Putative L-asparaginase	2.11
***cbpA* (HPYLSS1_00408)**	Curved DNA-binding protein	2.19
HPYLSS1_00252	Chaperone protein ClpB	2.7
HPYLSS1_01332	CMP-N-acetylneuraminate-beta-galactosamide	2.2
Amino acid biosynthesis		
***porC* (HPYLSS1_01050)**	Pyruvate synthase subunit PorC	2.02
Fatty acid and phospholipid metabolism		
***acpS* (HPYLSS1_00527)**	Holo-[acyl-carrier-protein] synthase	2.89
***fenF* (HPYLSS1_00085)**	Malonyl CoA-acyl carrier protein transacylase	2.26
Biosynthetic of cofactors, prosthetic groups and carriers		
***thiE* (HPYLSS1_00492)**	Thiamine-phosphate synthase	4.13
***salL* (HPYLSS1_00914)**	Adenosyl-chloride synthase	2.87
DNA restriction, modification, recombination, and repair		

HPYLSS1_00696	Restriction endonuclease	2.19
Transport and binding proteins		
***metI* (HPYLSS1_01522)**	D-methionine transport system permease protein	2.18
HPYLSS1_00805	Putative ABC transporter ATP-binding protein	2.02
Energy metabolism		
***ansA* (HPYLSS1_00615)**	Putative L-asparaginase	2.11
HPYLSS1_00772	Pyrroloquinoline quinone biosynthesis protein	7.5
Hypothetical proteins		
HPYLSS1_00605	hypothetical protein/Putative GTPase dynamin	17.63
HPYLSS1_00355	Hypothetical protein	7.82
HPYLSS1_01063	Hypothetical protein	7.58
HPYLSS1_00488	Hypothetical protein	5.65
HPYLSS1_01091	Hypothetical protein	5.34
HPYLSS1_00197	Hypothetical protein	4.4
HPYLSS1_00109	Hypothetical protein	4.25
HPYLSS1_00933	Hypothetical protein	3.91
HPYLSS1_01183	Hypothetical protein	3.37
HPYLSS1_00583	Hypothetical protein	3.07
HPYLSS1_00404	Hypothetical protein	2.85
HPYLSS1_01474	Hypothetical protein	2.77
HPYLSS1_00984	Hypothetical protein	2.56
HPYLSS1_01009	Hypothetical protein	2.26
HPYLSS1_01271	Hypothetical protein	2.05
HPYLSS1_00558	Hypothetical protein	2.04
HPYLSS1_01019	Hypothetical protein	2.03
HPYLSS1_00777	Hypothetical protein	2.01
HPYLSS1_00529	Hypothetical protein	2

Table 3. Down-regulated genes in *H. pylori* SS1 biofilm (cutoff ratio ≤ -1 log2 fold change and p-value <0.05) using RNA-seq analysis, grouped by functional role categories.

Locus Name	Putative identification	Fold Change
Cell envelope		
***murB* (HPYLSS1_01344)**	UDP-N-acetylenolpyruvoylglucosamine reductase	-2.52
***fliM* (HPYLSS1_00401)**	Flagellar motor switch protein FliM	-2.25
***fliI* (HPYLSS1_01346)**	Flagellum-specific ATP synthase	-2.16
***yohD-1* (HPYLSS1_00775)**	Inner membrane protein YohD	-2.14
Cellular process		
***mreB* (HPYLSS1_01316)**	Rod shape-determining protein MreB	-2.95
***urea* (HPYLSS1_00068)**	Urease subunit alpha	-2.28
***groEL* (HPYLSS1_00013)**	60 kDa chaperonin	-2.17
***hcpC* (HPYLSS1_01039)**	Cysteine rich protein HcpC	-3.78
***cmmA* (HPYLSS1_01486)**	Polymer-forming cytoskeletal family protein	-2.58
***typA* (HPYLSS1_00442)**	GTP-binding protein	-2.02
Regulatory functions		
***hslV* (HPYLSS1_00733)**	ATP-dependent protease subunit	-3.33
HPYLSS1_00758	Putative TrmH family tRNA/rRNA	-2.24
Translation		
***rplR* (HPYLSS1_01253)**	50S ribosomal protein L18	-3.09
***rpsE* (HPYLSS1_01252)**	30S ribosomal protein S5	-3.06
***rpsG* (HPYLSS1_01140)**	30S ribosomal protein S7	-2.52
***rpsC* (HPYLSS1_01262)**	30S ribosomal protein S3	-2.49
***rpsK* (HPYLSS1_01246)**	30S ribosomal protein S11	-2.44
***rplW* (HPYLSS1_01266)**	50S ribosomal protein L23	-2.29
***rplN* (HPYLSS1_01258)**	50S ribosomal protein L14	-2.29
***rplD* (HPYLSS1_01267)**	50S ribosomal protein L4	-2.23

***rplB* (HPYLSS1_01265)**	50S ribosomal protein L2	-2.22
***rplF* (HPYLSS1_01254)**	50S ribosomal protein L6	-2.21
***rpmF* (HPYLSS1_00189)**	50S ribosomal protein L32	-2.14
***rpsD* (HPYLSS1_01245)**	30S ribosomal protein S4	-2.12
***rplS* (HPYLSS1_01093)**	50S ribosomal protein L19	-2.09
***rplE* (HPYLSS1_01256)**	50S ribosomal protein L5	-2.07
***rplV* (HPYLSS1_01263)**	50S ribosomal protein L22	-2.02
***rpmG* (HPYLSS1_01151)**	50S ribosomal protein L33	-2.02
***fusA* (HPYLSS1_01139)**	Elongation factor G	-2.23
***tufa* (HPYLSS1_01152)**	Elongation factor Tu	-2.14
***yigZ* (HPYLSS1_01411)**	Elongation factor	-2.05
Amino acid biosynthesis		
***trpB* (HPYLSS1_01240)**	Tryptophan synthase beta chain	-2.68
Fatty acid and phospholipid metabolism		
***acpP_2* (HPYLSS1_00944)**	Acyl carrier protein	-2.96
***plsX* (HPYLSS1_00190)**	Phosphate acyltransferase	-2.71
***scoB* (HPYLSS1_00895)**	3-Oxoacid CoA-transferase, subunit B	-2.11
Biosynthetic of cofactors, prosthetic groups and carriers		
***birA* (HPYLSS1_01084)**	Bifunctional ligase/repressor BirA	-3.29
***ribH* (HPYLSS1_00002)**	6,7-dimethyl-8-ribityllumazine synthase	-2.47
***folK* (HPYLSS1_00396)**	2-amino-4-hydroxy-6-hydroxymethyldihydropteridine pyrophosphokinase	-2.13
***ggt* (HPYLSS1_01061)**	Gamma-glutamyl transpeptidase	-2.06
DNA restriction, modification, recombination, and repair		
HPYLSS1_00145	Recombinase A	-2.46
Energy metabolism		
***atpC* (HPYLSS1_01075)**	ATP synthase epsilon chain	-2.78
***atpE* (HPYLSS1_01164)**	ATP synthase subunit c	-2.48
***nifU* (HPYLSS1_00210)**	NifU-like protein	-2.15
***adhA* (HPYLSS1_00)**	Alcohol dehydrogenase	-2.12
***mdaB* (HPYLSS1_00836)**	Modulator of drug activity B	-2.05
Purine, pyrimidine, nucleosides and nucleotide		
***pyrD_2* (HPYLSS1_01468)**	Dihydroorotate dehydrogenase B (NAD(+)), catalytic subunit	-2.13

Hypothetical proteins		
HPYLSS1_00188	Hypothetical protein	-3.92
HPYLSS1_00885	Hypothetical protein	-3.15
HPYLSS1_00325	Hypothetical protein/Putative beta-lactamase	-2.95
HPYLSS1_00036	Hypothetical protein/Putative Nucleoid-associated protein	-2.79
HPYLSS1_01458	Hypothetical protein	-2.79
HPYLSS1_01225	Hypothetical protein	-2.71
HPYLSS1_00259	Hypothetical protein	-2.66
HPYLSS1_01321	Hypothetical protein	-2.44
HPYLSS1_01060	Hypothetical protein	-2.32
HPYLSS1_00657	Hypothetical protein	-2.27
HPYLSS1_01143	Hypothetical protein	-2.21
HPYLSS1_00296	Hypothetical protein/Putative F0F1-ATPase subunit	-2.2
HPYLSS1_00945	Hypothetical protein	-2.16
HPYLSS1_00057	Hypothetical protein	-2.03
HPYLSS1_00569	Hypothetical protein	-2.07

759

760

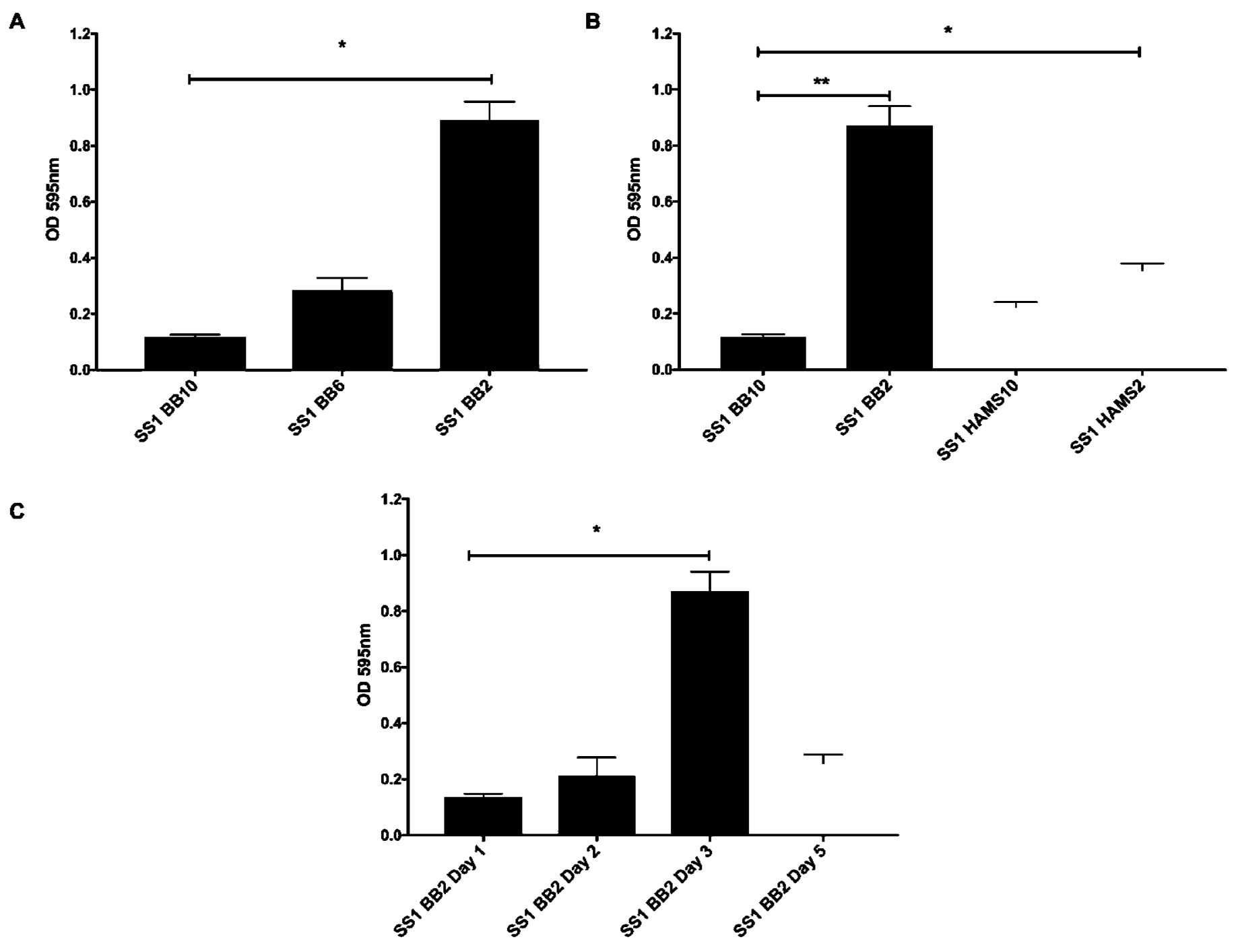
A
OD 595nm
1.2
1.0
0.8
0.6
0.4
0.2
0.0
*
SS1 BB10
SS1 BB6
SS1 BB2
B
OD 595nm
1.2
1.0
0.8
0.6
0.4
0.2
0.0
*
**
SS1 BB10
SS1 BB2
SS1 HAMS10
SS1 HAMS2
C
OD 595nm
1.2
1.0
0.8
0.6
0.4
0.2
0.0
*
SS1 BB2 Day 1
SS1 BB2 Day 2
SS1 BB2 Day 3
SS1 BB2 Day 5

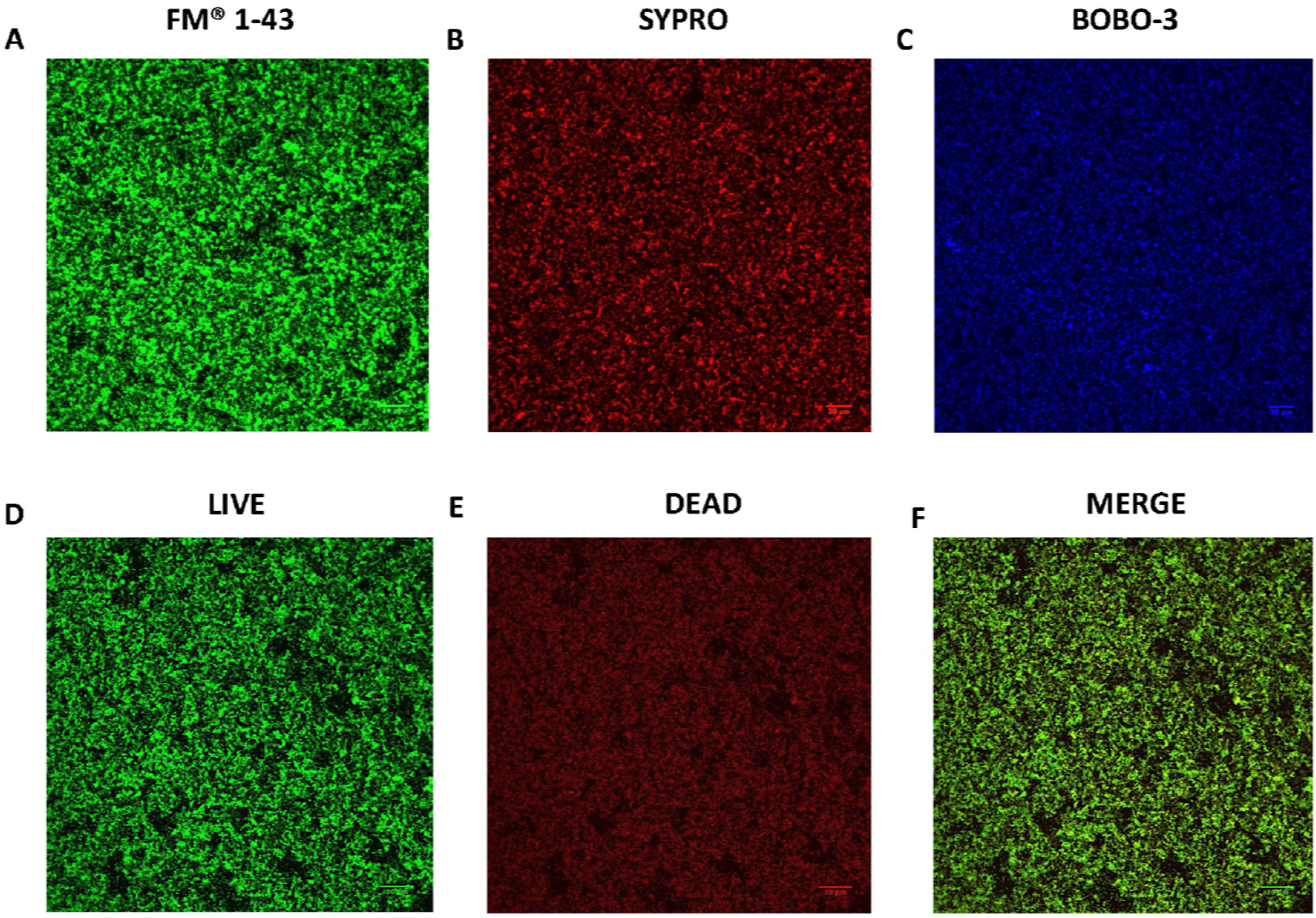

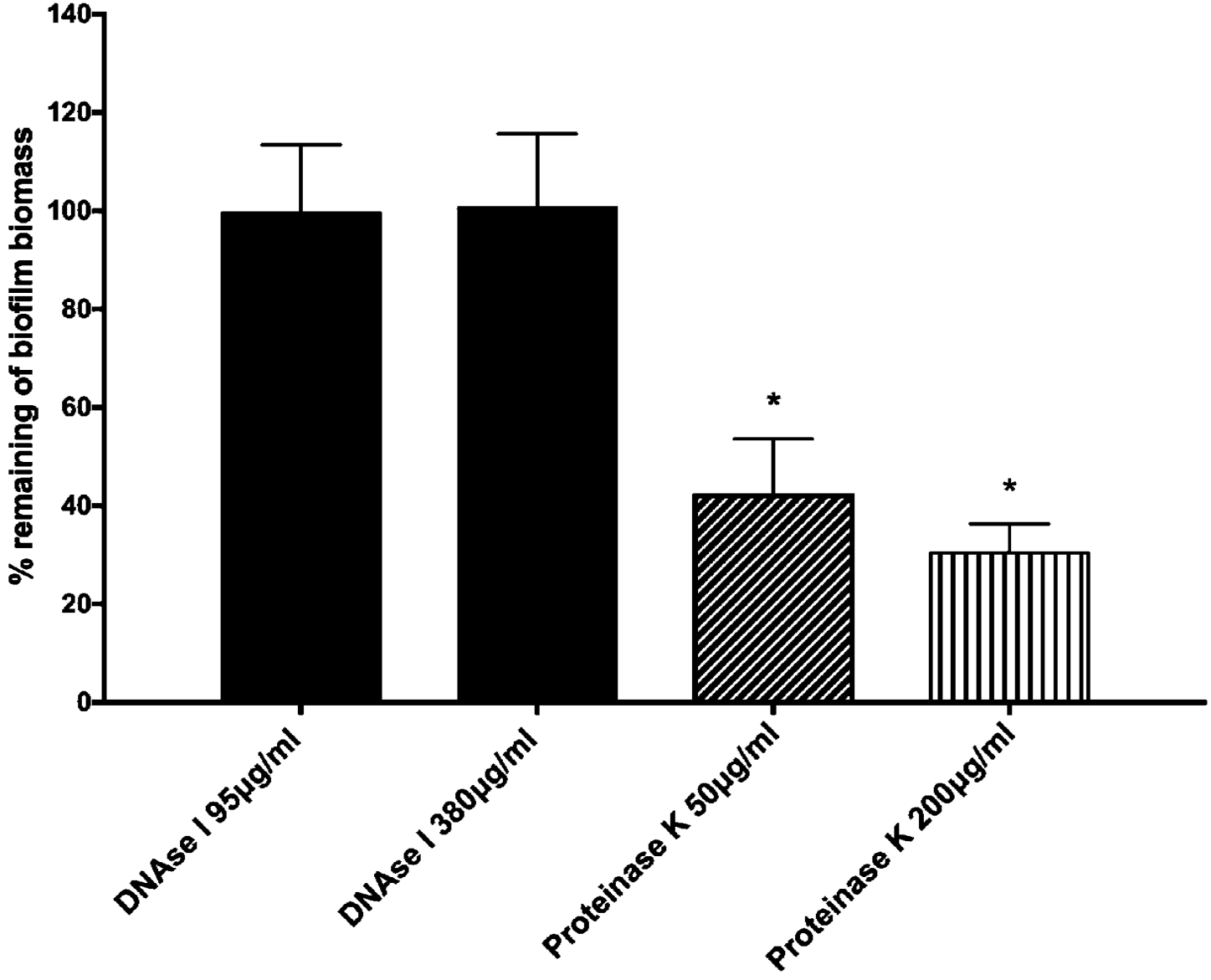
140
120
100
80
60
40
20
0
% remaining of biofilm biomass
*
*
DNAse I 95µg/ml
DNAse I 380µg/ml
Proteinase K 50µg/ml
Proteinase K 200µg/ml

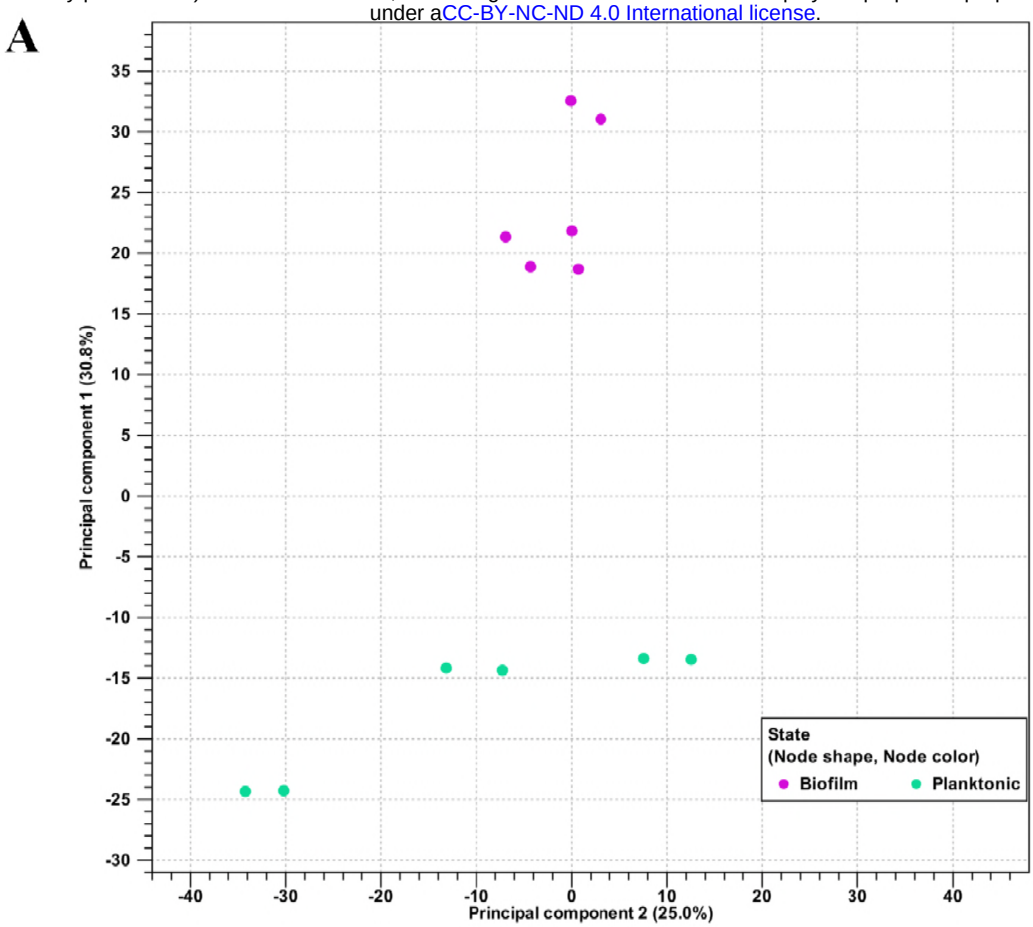

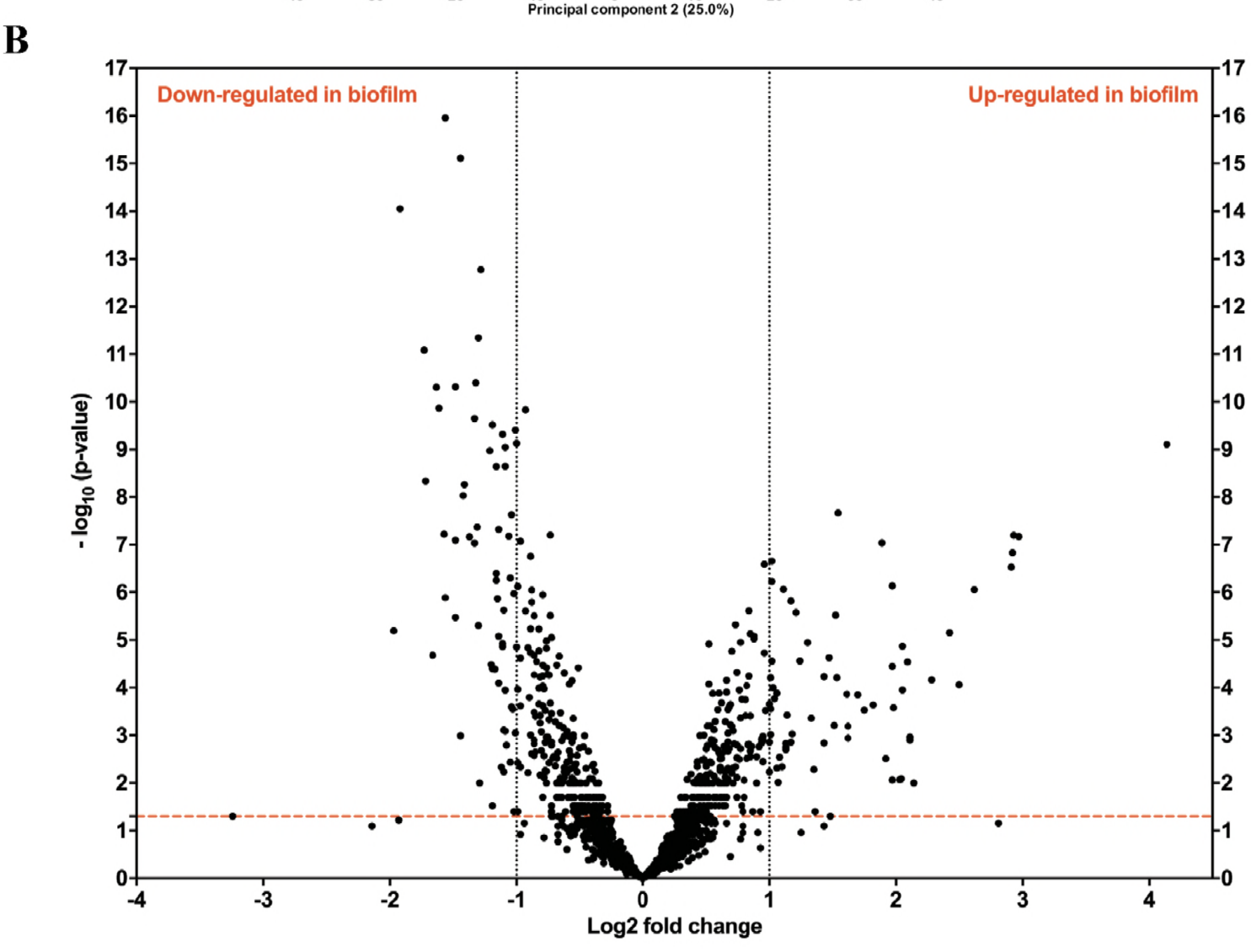

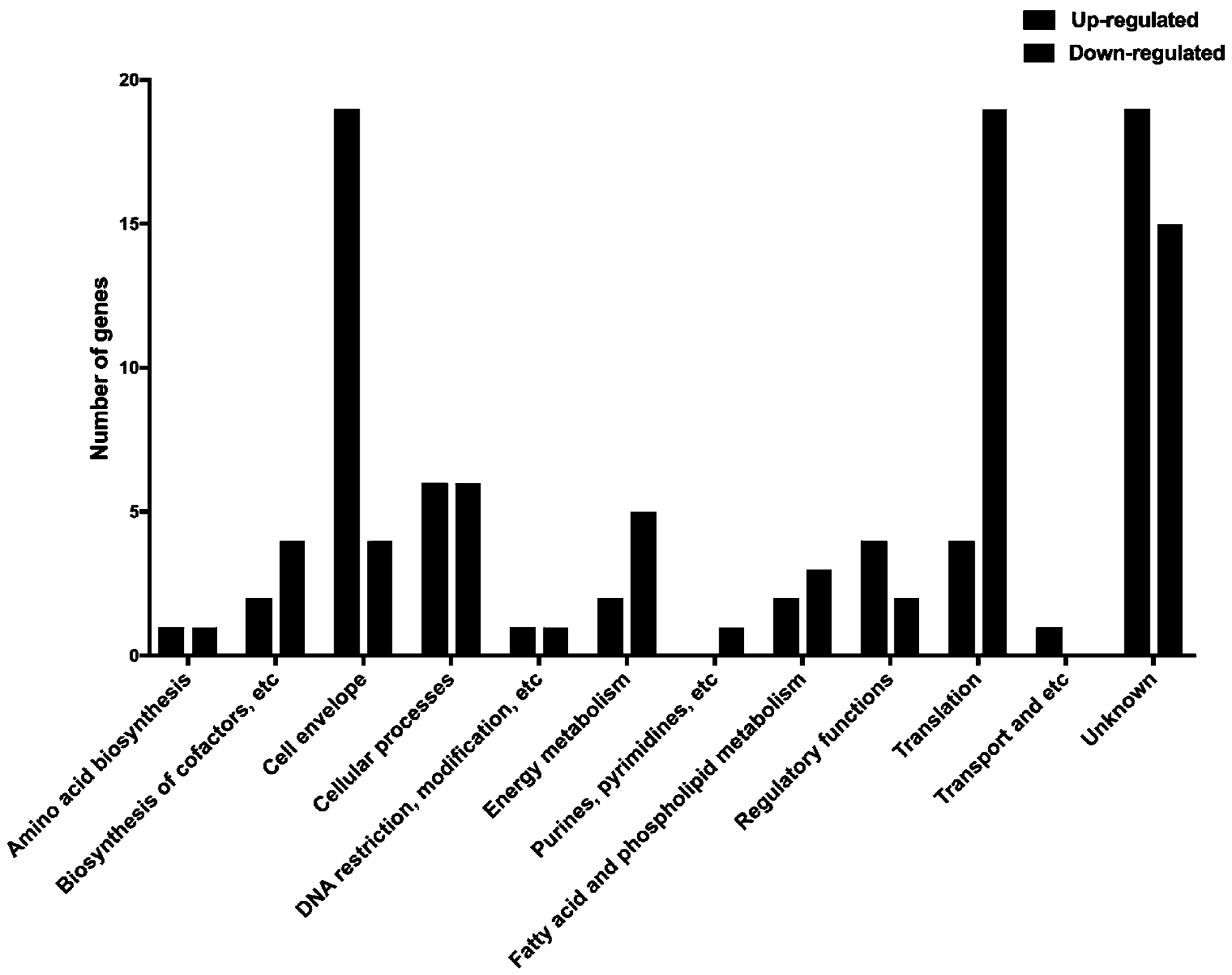
Up-regulated
Down-regulated
Number of genes
20
15
10
5
0
Amino acid biosynthesis
Biosynthesis of cofactors, etc
Cell envelope
Cellular processes
DNA restriction, modification, etc
Energy metabolism
Purines, pyrimidines, etc
Fatty acid and phospholipid metabolism
Regulatory functions
Translation
Transport and etc
Unknown

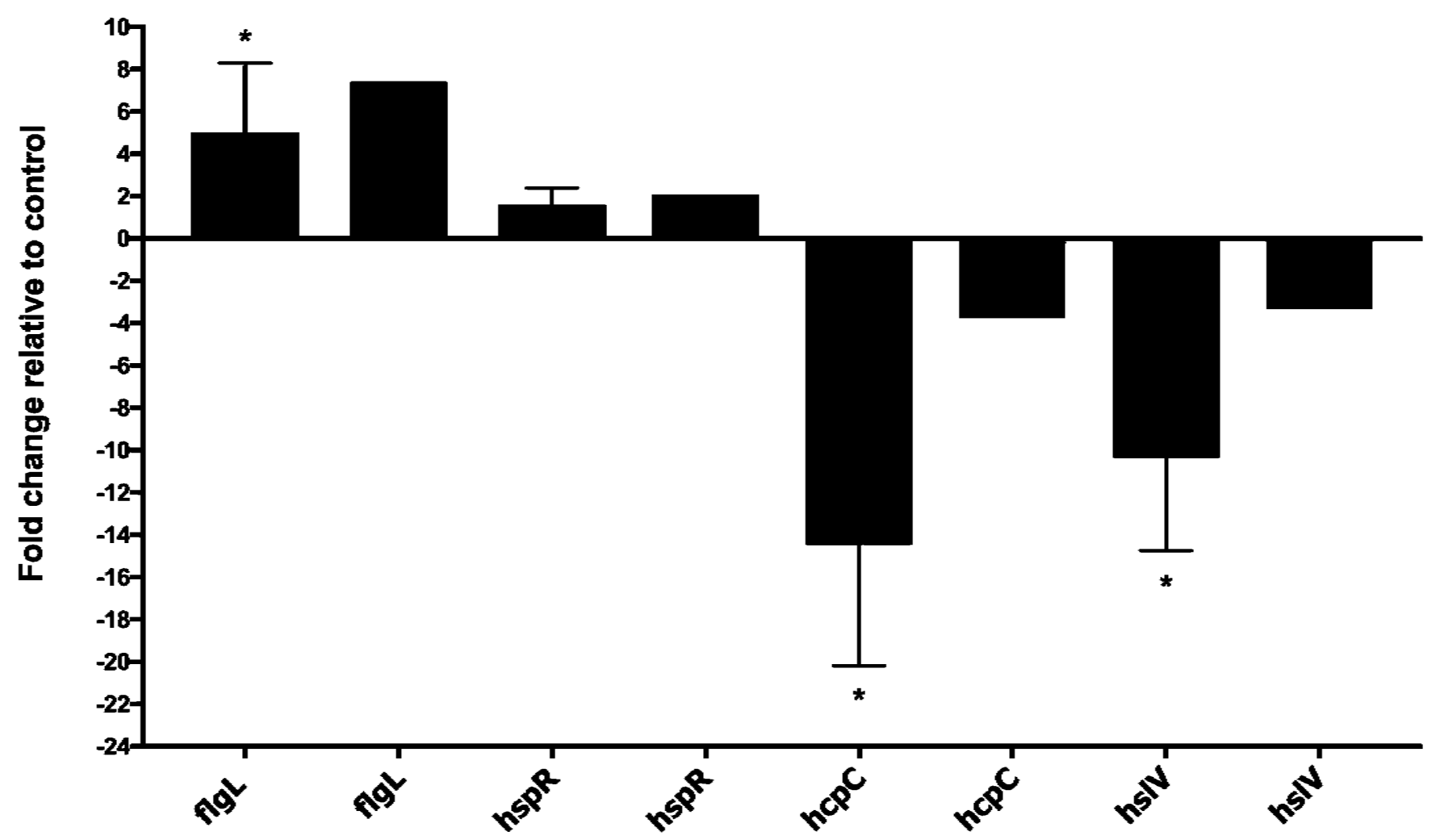
Fold change relative to control
10
8
6
4
2
0
-2
-4
-6
-8
-10
-12
-14
-16
-18
-20
-22
-24
*
*
*
flgL
flgL
hspR
hspR
hcpC
hcpC
hslV
hslV

A

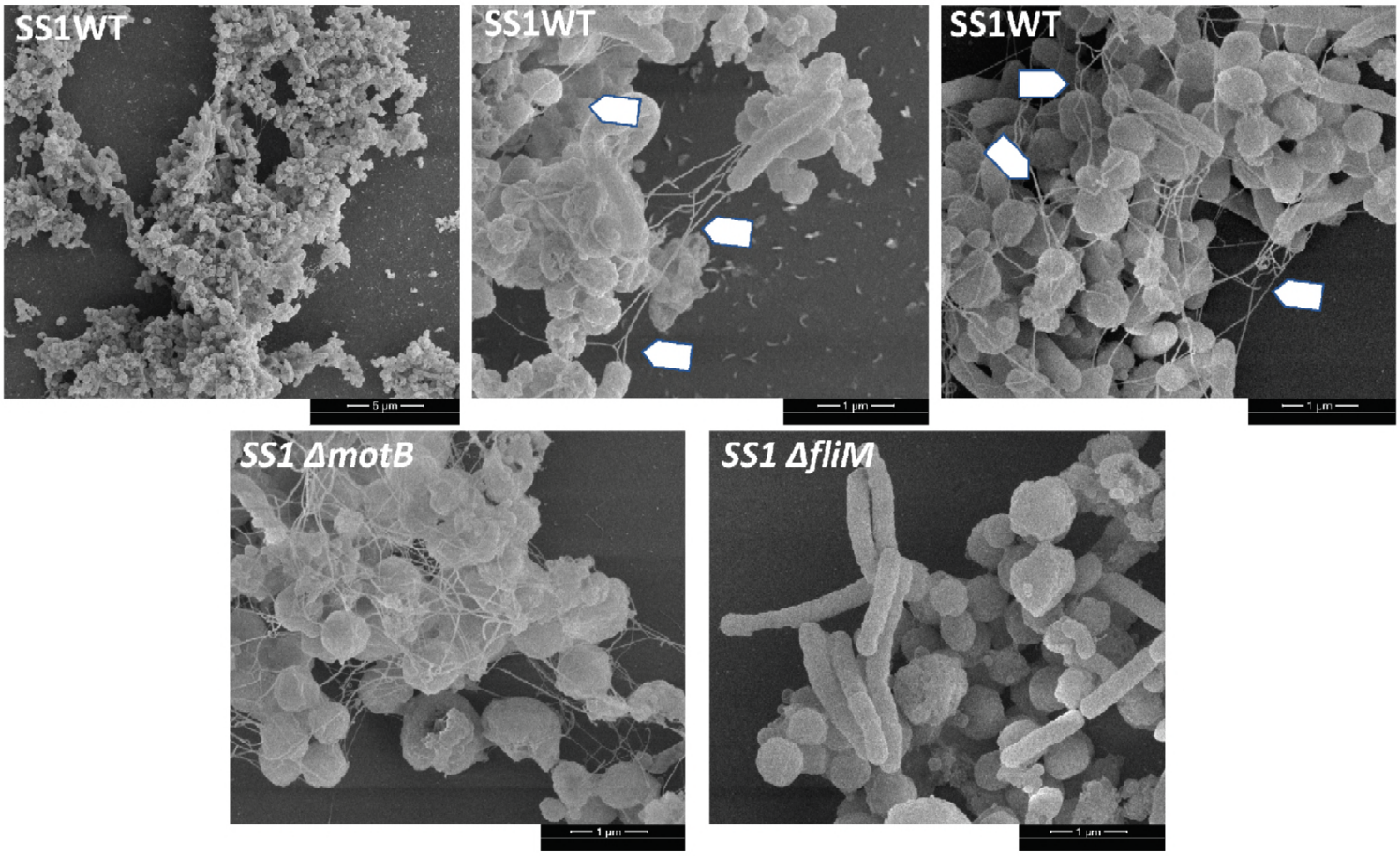

B

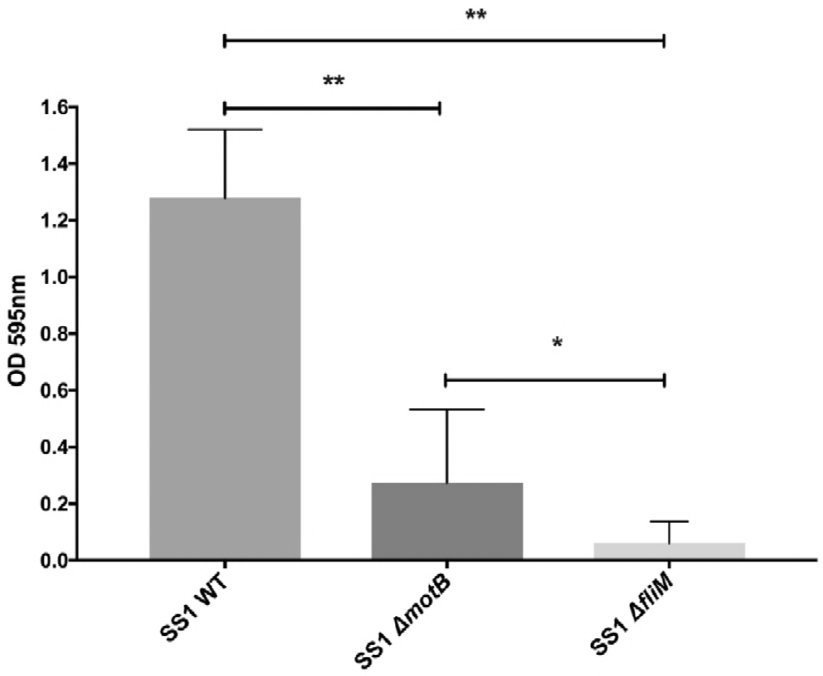

A

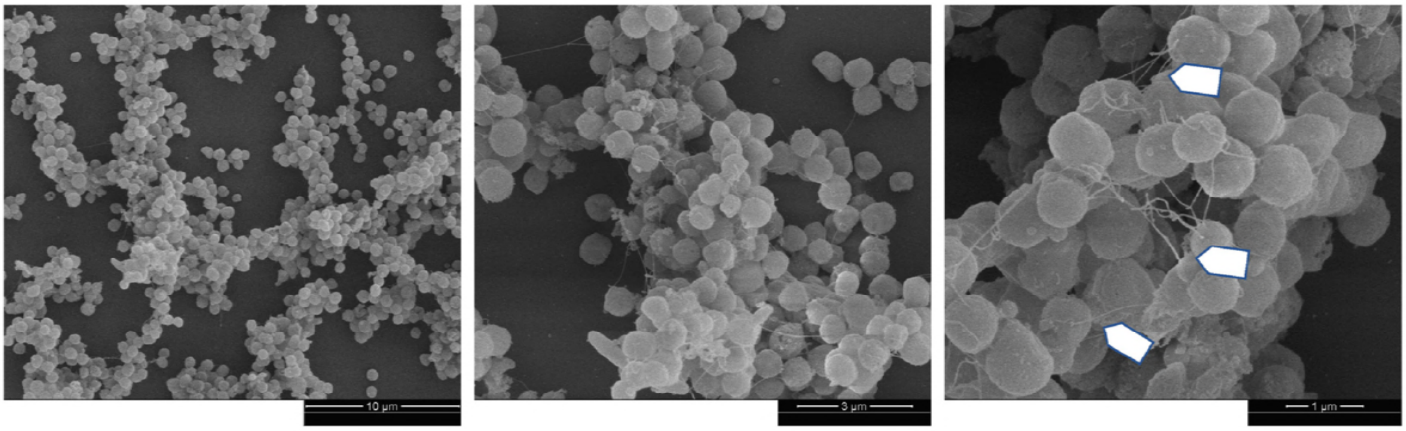

B